Accepted manuscript version

ChemPhysChem 2013, volume 14, pages 3355–3360

DOI for the Published journal article (PJA) is 10.1002/cphc.201300503

Self-assembly structures of 1*H*-indazoles in solution and solid phases: A vibrational (IR, FarIR, Raman and VCD) and computational study.

J. R. Avilés Moreno,[a] M. M. Quesada Moreno, [a] J. J. López González,*[a] R. M. Claramunt,*[b] C. López, [b] I. Alkorta[c] and J. Elguero*[c]

[a] *Departamento de Química Física y Analítica, Universidad de Jaén, Campus Las Lagunillas, E-23071 Jaén, Spain*
E-mail: jjlopez@ujaen.es

[b] *Departamento de Química Orgánica y Bio-Orgánica, Facultad de Ciencias, Universidad Nacional de Educación a Distancia (UNED), Senda del Rey 9, E-28040 Madrid, Spain*
E-mail: rclaramunt@ccia.uned.es

[c] *Instituto de Química Médica (CSIC), Juan de la Cierva, 3,E-28006 Madrid, Spain*
E-mail: iqmbe17@iqm.csic.es

Abstract: 1*H*-indazoles are good candidates to study phenomena of molecular association and spontaneous resolution of chiral compounds. Thus, because the 1*H*-indazoles can crystallize forming dimers, trimers or catemers, depending on their structure and the phase where they are, the difficulty of the experimental analysis of the structure of the family of 1*H*-indazoles is clear. This lead to contemplate several questions: How can we determine the presence of different structures of a determined molecular species if they change according to the phase? Could these different structures be present in the same phase simultaneously? How can it be determined? In order to shed light on these questions, we outline a very complete strategy by using different techniques of vibrational spectroscopy sensitive (VCD) and not sensitive (IR, FarIR and Raman) to the chirality together with quantum chemical calculations.

1. Introduction and motivations

1*H*-indazoles are good candidates to study phenomena of molecular association and spontaneous resolution of chiral compounds [1]. In those cases where the N-H···N hydrogen bonds between 1 and 2 (see Scheme 1) determine the secondary structure, indazoles crystallize forming dimers, trimers or catemers (chains) [2]. When the monomer is achiral, the most common case is that the crystal is also achiral, being usually a dimer or a trimer. An example of this group is 3-methyl-1*H*-indazole, **LIDFUA** (code used by the CSD to identify the compounds [3]) in the solid state (see Scheme 1) crystallizing as a dimer [4]. If it is a catemer, an achiral structure can be obtained if two helices of opposing chirality are present in the unit cell, for example in **TELXUD** (space group *Pbca*) [5]

On the other hand, 3-trifluoromethyl-4,5,6,7-tetrafluoro-1*H*-indazole, **LIDGEL** (see Scheme 1), is an example of 1*H*-indazole crystallizing as a catemer where only one enantiomer is present in the unit cell for a given crystal that can be separated manually, *i.e.* they are conglomerates (spontaneous resolution) [1,2]. The subject of spontaneous resolution of achiral molecules is very relevant because it is related with the origin of the life [1,2,6].

Vibrational circular dichroism (VCD) spectroscopy has shown to be a very useful tool for studying the chirality in both molecular species in solution [7] and supramolecular organizations in solid phase [8]. Moreover, combined with quantum chemical calculations, it has allowed the determination of absolute configurations in both cases [6]. Particularly, in ref [5] the chirality, and further the absolute supramolecular configuration of the parent 1*H*-indazole crystals, **INDAZL**, in the solid state was obtained by using concomitantly X-ray and IR, Raman and VCD experimental data and quantum chemical calculations. In ref [9] the trimeric structure of the crystals of (4*S*,7*R*)-7,8,8-trimethyl-4,5,6,7-tetrahydro-4,7-methano-2*H*-indazole, **LABHEB**, in the solid state and its absolute configuration have also been determined using IR, Raman and VCD spectroscopies combined with DFT calculations.

Thus, because any 1*H*-indazole can in principle crystallize forming dimers, trimers or catemers depending on the phase where it is present, as above mentioned, the difficulty of the experimental analysis of the structure of the family of 1*H*-indazoles is clear. This lead to contemplate several questions: How can we determine the presence of different structures of a determined molecular species if they change according to the phase? Could these different structures be present in the same phase simultaneously? How can it be determined?

To try to answer those questions, and in addition to the studies carried out in refs [5] and [8] for **INDAZL** and **LABHEB** crystals, respectively, in this paper, we outline a very complete strategy by using different techniques of vibrational spectroscopy sensitive (VCD) and not sensitive (IR, FarIR and Raman) to the chirality together with quantum chemical calculations.

The determination of the absolute configuration of chiral compounds and crystalline supramolecular organizations requires the comparison of the experimental VCD spectra of a pair of enantiomorphous species and crystals, respectively, with the calculated VCD spectrum for one enantiomer. The case of enantiomers (*R*, *S*) is much simpler than that of helices (*M*, *P*) because it is suffices to calculate the corresponding monomer or oligomer. If the chirality appears in the secondary structure, it is further necessary to calculate catemers with increasing number of monomers until the experiment becomes acceptably reproduced [5].

In addition, in order to carry out the interpretation of the VCD spectral features of medium size chiral compounds, our experience reveals that a previous vibrational analysis for them, from IR and Raman data and quantum chemical calculations, is a recommended approach [6].

2. Results and discussion

Vibrational absorption spectra

Our methodology for the systematic study of 3-methyl-1*H*-indazole and 3-trifluoromethyl-4,5,6,7-tetrafluoro-1*H*-indazole in liquid and solid phases will be: *1)* Recording the IR spectra in CCl_4 of 3-methyl-1*H*-indazole and 3-trifluoromethyl-4,5,6,7-tetrafluoro-1*H*-indazole. *2)* Recording the IR (including FarIR) and Raman spectra in solid phase of **LIDFUA** and **LIDGEL** crystals. *3)* Then, these spectra will be compared with the calculated B3LYP/6-31G(d) spectra of the monomers and the oligomers (see Figure 1) of both chemical species, after using a frequency scale factor of 0.96 [10]. DFT calculations have been done in the harmonic approximation in this work; it does not consider overtones and combination bands, therefore, some bands of IR and Raman spectra are not predicted here. *4)* Recording the IR and VCD spectra of **LIDFUA** and **LIDGEL** crystals in nujol/fluorolube mulls. *5)* The VCD spectra of LIDGEL will be compared with those calculated at the B3LYP/6-31G(d) level for the monomer and oligomers of these chemical species. This approach has not been used for **LIDFUA** crystals because their samples are VCD-silent, as expected of its achirality and of the centrosymmetric character of its crystals.

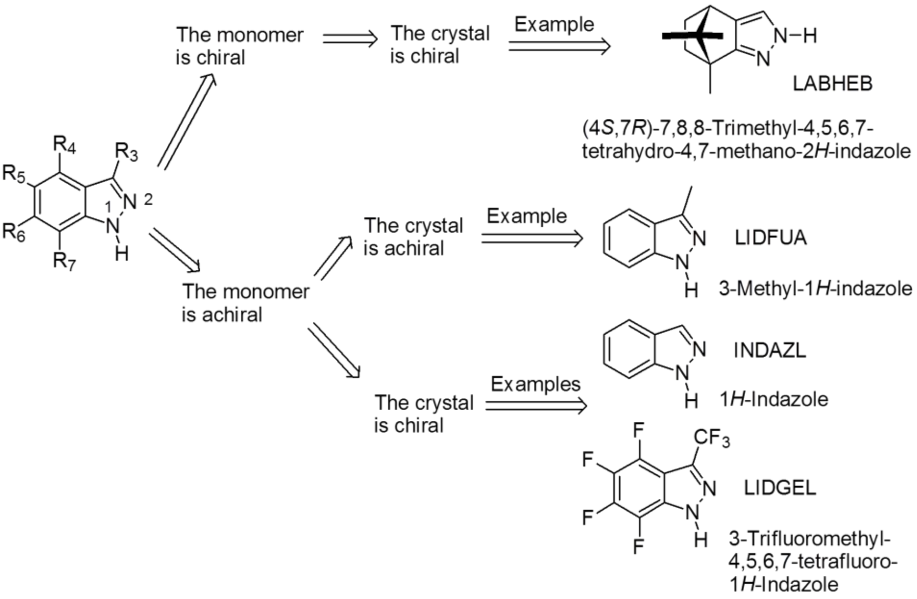

Scheme 1. The different situations present in crystals of N*H*-indazoles with their refcodes [3].

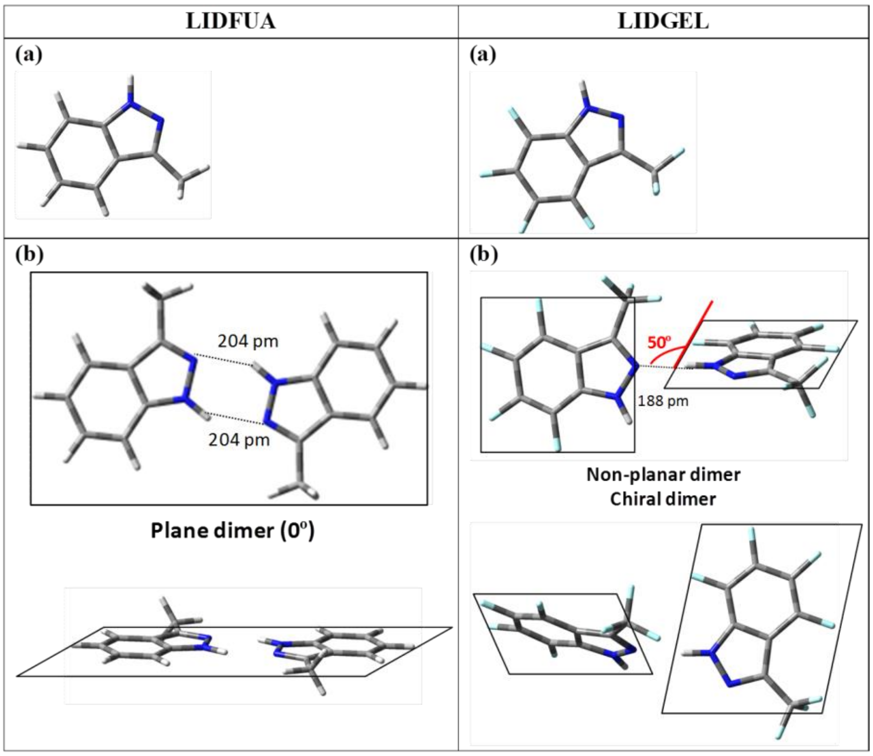

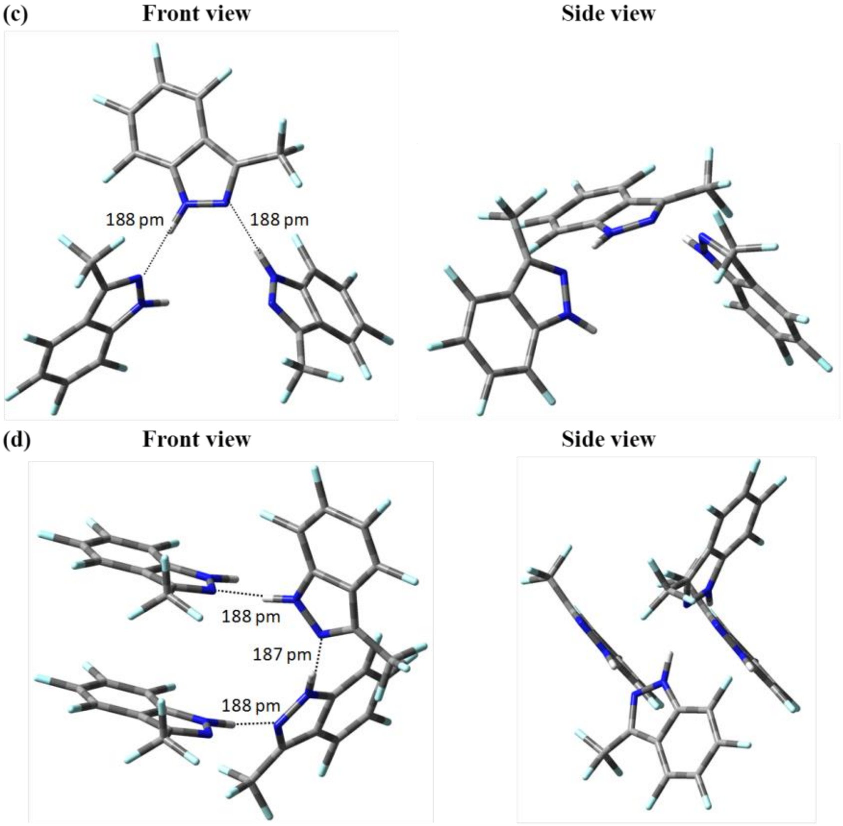

Figure 1. Molecular structures of **LIDFUA** and **LIDGEL** monomers and oligomers.

We have started to analyze the presence of different structures of 3-methyl-1*H*-indazole and 3-trifluoromethyl-4,5,6,7-tetrafluoro-1*H*-indazole focusing our attention on their Raman and IR spectra, *i.e.* N-H stretching, C-H stretching and intermediate regions (see SI). In the experimental IR spectra in CCl_4 solution of the two *NH*-indazoles (3-methyl-1*H*-indazole and 3-trifluoromethyl-4,5,6,7-tetrafluoro-1*H*-indazole), the monomer as well as the achiral dimer (3-methyl-1*H*-indazole) or chiral oligomers (3-trifluoromethyl-4,5,6,7-tetrafluoro-1*H*-indazole) seems to be present. However, the presence of the associated species of both compounds seems to be enough to reproduce the experimental FarIR and Raman spectra in the solid phase (**LIDFUA** and **LIDGEL** crystals).

The low frequency region is very useful in order to differentiate between different structures of **LIDFUA** (see Figure 2a) and **LIDGEL** (see Figure 2b). The experimental FarIR and Raman spectra of **LIDFUA** solid are in good agreement with the theoretical ones of the achiral monomer and dimer structures, but the dimer model better predicts them. Furthermore, the experimental FarIR and Raman spectra of **LIDGEL** are in better agreement with the theoretical ones of the tetramer model.

This region, with vibrations below 700 cm^{-1}, presents bands corresponding to normal modes with contributions of waggings, rockings and torsions (see Figure 2a and 2b). In the first place, Figure 2a displays some examples of them, such as the experimental bands at 585 cm^{-1} (IR, 574 cm^{-1} in Raman) and at 532 cm^{-1} (IR and Raman) that are assigned to the ring deformation of **LIDFUA** structure. Another interesting band is observed at 468 cm^{-1} (IR, 474 cm^{-1} in Raman) and is assigned to ring deformation. This last band is due to presence of dimers. In addition, the experimental band at 239 cm^{-1} (IR and Raman) is assigned to the butterfly motion. Another example is the band observed at 189 cm^{-1} (IR, 191 cm^{-1} in Raman), which is assigned to torsion normal modes of one **LIDFUA** subunit with respect to the other one.

In the second place, we can make remarks about the most helpful and relevant spectral features of Figure 2b. An example of them is the experimental band observed at 492 cm^{-1} (IR and Raman), which corresponds to the asymmetric ring deformation of **LIDGEL** structure. Other examples are the bands observed at 319 cm^{-1} (IR and Raman), at 294 cm^{-1} (IR and Raman) and at 268 cm^{-1} (IR, 269 cm^{-1} in Raman), which are assigned to the C-H rocking normal modes of the benzene and pyrazole rings. These four bands are due to presence of oligomers. Another example could be the experimental band observed at 193 cm^{-1} (IR and Raman), which is assigned to the butterfly motion.

Finally, in both Figures (2a and 2b), due to the fact that the 3-methyl-1*H*-indazole and 3-trifluoromethyl-4,5,6,7-tetrafluoro-1H-indazole monomer structures does not present any band below 170 cm^{-1}, the two bands present in the Far-IR and Raman spectra of the solid **LIDFUA** at 80 cm^{-1} (IR, broad band at 103 cm^{-1} in Raman) and at 55 cm^{-1} (IR), and the three bands present in the Far-IR and Raman spectra of the solid **LIDGEL** at 132 cm^{-1} (IR and Raman), at 117 cm^{-1} (IR and Raman) and at 82 cm^{-1} (IR, 84 cm^{-1} in Raman) can be assigned to more complex molecular species, *i.e.* oligomers. Concretely, the theoretical Far-IR and Raman spectra calculated for the dimer configuration of **LIDFUA** and for dimer, trimer and tetramer configurations of **LIDGEL** allow the following assignment:

In the case of **LIDFUA**, the first band (80 cm^{-1}) is assigned to the methyl torsions of the two monomers subunits and the second one (55 cm^{-1}) to torsion normal modes of one subunit with respect to the other one. The first band (132 cm^{-1}) of **LIDGEL** is assigned to the butterfly motion, the second band (117 cm^{-1}) to the framework deformation and the third one (82 cm^{-1}) to torsion normal modes of one **LIDGEL** subunit with respect to the others.

The other spectral regions (see Figure 1S) in both IR and Raman spectra, *i.e.*: N-H, C-H and intermediate regions agree with the presence of the above-mentioned structures for 3-methyl-1*H*-indazole and 3-trifluoromethyl-4,5,6,7-tetrafluoro-1*H*-indazole species.

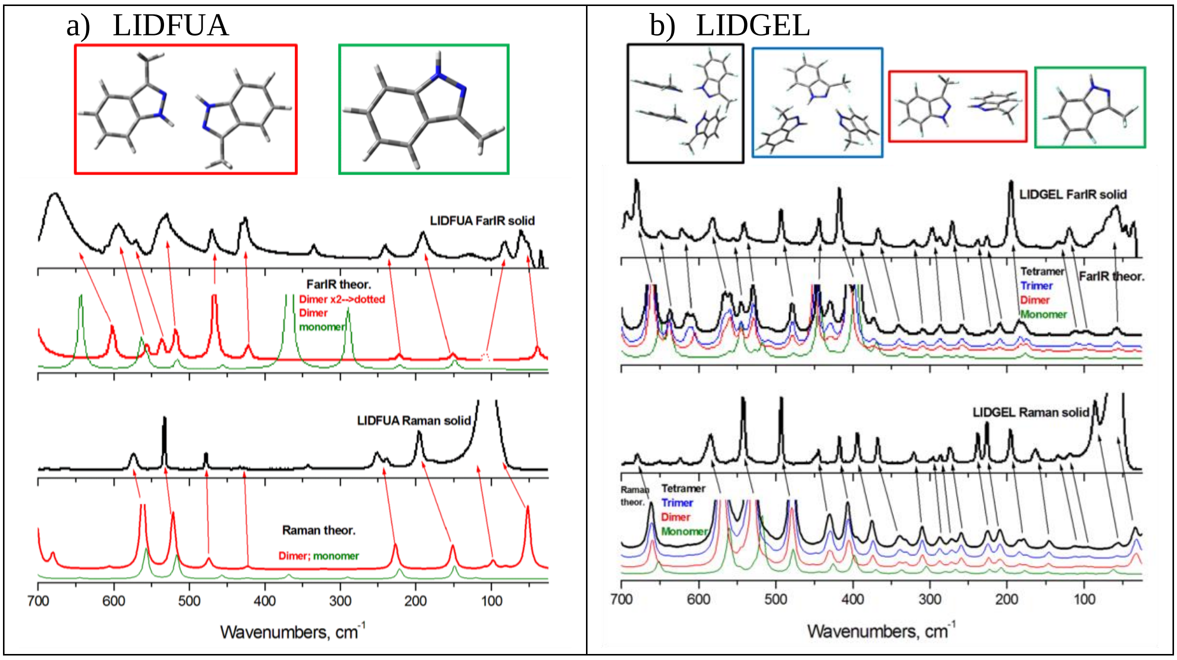

Figure 2. Experimental and scaled predicted Far-IR and Raman spectra of **LIDFUA** (panel a) and **LIDGEL** (panel b) in the 700 cm^{-1}–25 cm^{-1} spectral region.

Chirooptical response

Up to now, the vibrational (IR-Raman) study has been made taking into account the presence of monomer, dimer, trimer and tetramer species in the 3-trifluoromethyl-4,5,6,7-tetrafluoro-1*H*-indazole and the monomer and dimer species in the 3-methyl-1*H*-indazole molecule. In the case of **LIDGEL** crystals, the analysis of the VCD spectra, shown below, will throw more light on this matter, especially on the configuration M (RRRR. . .) or P (SSSS. . .) of the **LIDGEL** catemer.

Now, we can examine the chirooptical properties of **LIDGEL** in relation with their structures in the different phases by means of the combined use of vibrational circular dichroism (VCD) and computational calculations [11]. In this way, the signs of the rotatory strength will be helpful to determine the absolute configuration of the **LIDGEL** catemer *i.e.*, P or M helix model. In addition, the VCD-silent character of the samples of **LIDFUA** crystals helps us to confirm the achirality of its structures present in the solid phase (see Figure 2S).

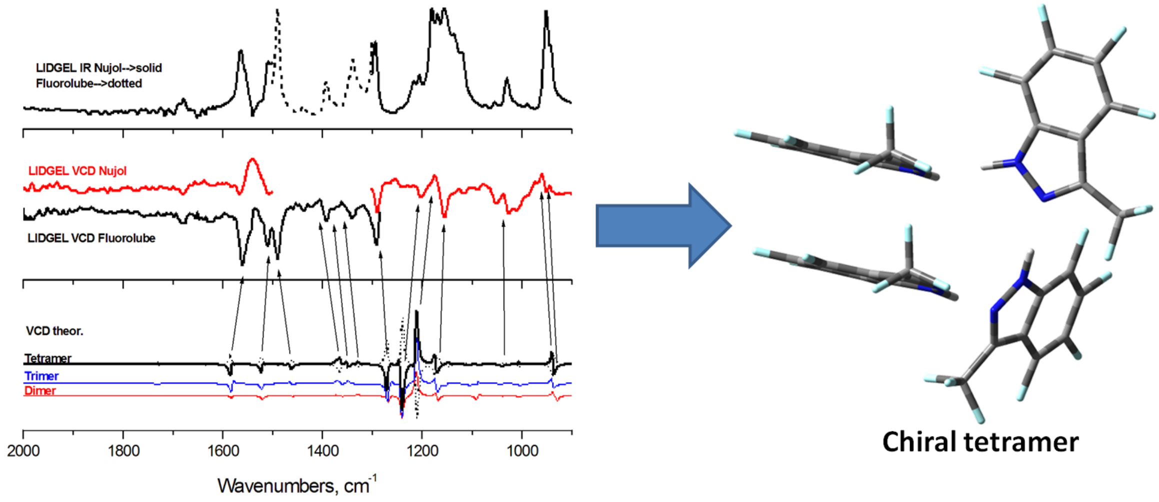

Figure 3. Experimental IR spectra (top) and experimental (middle) and theoretical (bottom) VCD spectra of **LIDGEL** in the 2000 cm^{-1}–900 cm^{-1} spectral region.

LIDGEL crystallizes as catemers. Thus, it is expected that only **LIDGEL** presents a chirooptical response, *i.e.* VCD features in solid state. Figure 3 displays the experimental (in fluorolube/nujol mulls) IR and VCD spectra and theoretical VCD spectra of **LIDGEL** crystals in the 2000-900 cm^{-1} spectral region. Data concerning the Raman spectra in solid phase in the 2000-400 cm^{-1} region are also shown in Figure 1S. Bottom panel in Figure 3 shows the predicted scaled VCD spectra for the **LIDGEL** dimer (in red), trimer (in blue) and tetramer (in black), where the solid lines correspond to the S configuration (P helix model) and the dotted lines correspond to the R configuration (M helix model). The DFT calculations are made in the harmonic approximation.

We observe a fair agreement between the experimental VCD spectra and the predicted scaled ones for **LIDGEL** (see Figure 2). A few experimental VCD bands that evidence the presence of a chiral structure are:

(1) In fluorolube mulls, the three (–, –, –) bands at 1560, 1510 and at 1490 cm^{-1} are well predicted by the dimer and trimer models, but better predicted by the tetramer model (*P* helix model). The bands observed at 1560 cm^{-1} (VCD, IR and Raman) and at 1510 cm^{-1} (VCD, 1506 cm^{-1} in IR and Raman) are assigned to the C-N and C=C (aromatic) bond stretchings of the pyrazole ring. In addition, the experimental band observed at 1490 cm^{-1} (VCD and IR, 1497 cm^{-1} in Raman) is assigned to the N-H wagging normal mode.

(2) Concerning the VCD spectra in nujol mulls, we can assign the region below 1400 cm^{-1} in fair agreement with the predicted VCD spectra: once again, the tetramer model (P helix, *(S)* configuration) improves the agreement with the experimental one in relation to the dimer and trimer models. For example, the (–) band observed at 1289 cm^{-1} (VCD, IR and Raman) is assigned to the rings deformation. Other interesting (–, +) bands are observed at 1194 cm^{-1} (VCD and IR, 1210 cm^{-1} in Raman) and at 1172 cm^{-1} (VCD and IR, 1163 cm^{-1} in Raman), being assigned to

the asymmetric CF_3 bending. A last example could be the (–) band observed at 1150 cm^{-1} (VCD and IR), which is assigned to the ring deformation.

3. Conclusions

1) We have measured the IR (including FarIR), VCD and Raman spectra of 3-methyl-1*H*-indazole and 3-trifluoromethyl-4,5,6,7-tetrafluoro-1*H*-indazole in solution as well as in the solid-state, and all bands, excluding overtones and combinations, were assigned based on scaled B3LYP/ 6-31G(d) calculations.

2) Although the dimer, trimer and tetramer models predict well the experimental VCD spectra of **LIDGEL** crystals, the last theoretical model improves the agreement with the experimentally recorded spectra. In order to get a better agreement between the experimental VCD spectra and the theoretical one we would need probably to improve the simulation of the helix model with calculations for an oligomer structure higher than those studied in this work. The reader interested in how the assignments were made in similar situations can refer to refs. [12] and [13] and, especially in the case of bonds involved in H-bonding, to ref. [14].

3) Concerning **LIDGEL** crystals, VCD technique allows the determination of its absolute configuration, *i.e*. *P* helix model. With the previous analysis of IR and Raman spectra we also concluded that different oligomers should be present CCl_4 solution depending on the concentration.

4) With the technique in hand, it should be possible to select a single crystal, increase its size by crystal growth and then determine its absolute configuration and its nonlinear optical properties.

5) In the case of 3-methyl-1*H*-indazole, achiral monomers and dimers seem to be present according to the experimental IR and Raman spectra in CCl_4 solution. However, the presence of dimers suffices to reproduce the experimental IR and Raman spectra in solid phase (**LIDFUA** crystals). The lack of chirooptical response was proved when its solution or mulls VCD spectra were recorded.

6) The analysis of the low frequency region (700-25 cm^{-1}) in the FT-Raman and Far-IR spectra reveals important information in order to determine the presence of the dimers (**LIDFUA**) or tetramers (**LIDGEL**) in the solid phase.

Experimental and theoretical details

Samples

3-Methyl-1*H*-indazole, **LIDFUA**, was prepared by treating *o*-ethylaniline with isoamyl nitrite as diazotizing agent in the presence of potassium acetate/acetic anhydride in toluene, followed by elimination of the acetyl group from the 1-acetylindazole thus formed [15]. White solid crystals of mp. 114-115 Cº were obtained from a solution of dichloromethane, plus hexane drops until dimness, at room temperature.

3-Trifluoromethyl-4,5,6,7-tetrafluoro-1*H*-indazole, **LIDGEL**, was prepared by reacting octafluoroacetophenone with hydrazine monohydrate as we have previously described in reference 4. White solid crystals of mp. 71-73 Cº were obtained from a solution of dichloromethane, plus hexane drops until dimness, at room temperature.

IR, Far-IR and Raman spectra

The Far-IR spectra of **LIDFUA** and **LIDGEL** in the solid phase were recorded using a Bruker Vertex 70 in the 700-25 cm^{-1} region, with a resolution of 4 cm^{-1} and 200 scans, and the platinum ATR accessory (single reflection diamond ATR accessory) and the silicon beamsplitter for the Far-IR region.

A FT-IR 4100 JASCO spectrometer, equipped with a Globar source, a DGTS detector and KBr optics, was used to record the IR spectra of 0.23 M, 0.11 M, 0.011 M, 0.0011M and 0.0023 M solutions (in CCl_4) using a standard liquid cell equipped with KBr windows. For the film spectra we prepare a very low concentration solution in CCl_4 of the sample and we evaporate the solvent under anhydrous conditions in order to get a very thin film of the sample which is measured. Finally, we have recorded the ATR spectra for the solid sample. The IR spectra have been recorded in the 4000–400 cm^{-1} range with a resolution of 1 cm^{-1} and 200 scans.

The Raman spectra of **LIDFUA** and **LIDGEL** have been recorded using a MultiRAM Stand Alone FT-Raman Spectrometer, equipped with an Nd:YAG laser (excitation line at 1064 nm) and a Ge detector cooled at liquid nitrogen temperature. The spectra were measured using a standard solid support with a resolution of 1 cm^{-1} and 200 scans.

VCD spectra

The VCD spectra of **LIDGEL** and **LIDFUA** in the fluorolube and nujol mulls were recorded using a JASCO FVS-4000 FTIR spectrometer, equipped with MCTV (2000–800 cm^{-1}) detector. A few milligrams of **LIDGEL** and **LIDFUA** were mixed with fluorolube or nujol mineral oils in order to get suitable mulls. Special attention is needed when working with solid samples in circular dichroism spectroscopy [16-18]. In fact, we have measured the mulls in several positions by rotating the sample around both the beam propagation axes (90º and 180º, face A) and that perpendicular to it (180º, face B) in order to get the true VCD peaks and to be sure on the absence of artifacts VCD spectra [18]. All spectra were recorded using a standard cell equipped with BaF_2 windows, with a resolution of 4–8 cm^{-1}, path lengths between 6–50 microns and 2000-8000 scans, by blocks of 2000 scans. Finally, the 0.28 M solution (in CCl_4) was also recorded. Concerning the baseline correction, we have subtracted the nujol and/or fluorolube signals for the suspension spectra and the solvent signal for the solution spectra.

Computational details

The geometry of the **LIDGEL** and **LIDFUA** monomers has been fully optimized while in the case of the dimer, trimer and tetramer, the position of the nonhydrogen atoms has been fixed at the positions determined by X-ray crystallography and hydrogen atoms have been optimized at the B3LYP/6-31G(d) [19,20] computational level . The vibrational analysis was carried out taking into account a single scaling factor of 0.960 from the NIST database for the B3LYP/6-31G(d) level. All the calculations have been carried out with the Gaussian package [21].

Acknowledgements

[*] This work has been supported by the Junta de Andalucía (project P08-FQM-04096). Authors thank the University of Jaén for continuing financial support and its CICT for instrumental facilities. Authors also thank the Ministerio de Ciencia e Innovación (Project Nos. CTQ 2009-13129-C02-02, CTQ2010-16122, CTQ2009-12520-C03-3, CTQ2012-35513-C02-02 and CONSOLIDER CSD2007-00041), the Comunidad Autónoma de Madrid (Project MADRISOLAR2, ref. S2009/PPQ-1533), for continuing support. Thanks are given to the CTI (CSIC) for the allocation of computer time. M^a del Mar Quesada Moreno thanks the University of Jaén of a predoctoral fellowship.

Keywords: chiral spontaneous resolution, chirality, secondary structure, hydrogen bond, DFT calculations, Vibrational Circular Dichroism

References

[1] a) A. G. Cairns-Smith, *Seven Clues to the Origin of Life*, Cambridge University Press, Cambridge, UK, **1985**; b) J. Jacques, A. Collet, S. H. Wilen, *Enantiomers, Racemates and Resolutions*, Krieger Publishing Company, Malabar, Florida, USA, **1994**; A. Guijarro, M. Yus, The Origin of Chirality in the Molecules of Life, RSC Publishing, Cambridge, UK, **2009**.

[2] C. Foces-Foces, *Acta Crystallogr. Sect. E: Struct. Rep. Online* **2005**, *61*, o337.

[3] a) Cambridge Structural Database, F. H. Allen. *Acta Crystallogr. Sect. B* **2002**, *58*, 380; b) F. H. Allen, W. D. S. Motherwell. *Acta Crystallogr. Sect. B* **2002**, *58*, 407; c) CSD version 5.32, updated Feb. **2011**. http://www.ccdc.cam.ac.uk

[4] J. Teichert, P. Oulié, K. Jacob, L. Vendier, M. Etienne, R. M. Claramunt, C. López, C. Pérez Medina, I. Alkorta, J. Elguero, *New J. Chem*. **2007**, *31*, 936.

[5] J. J. López González, F. Partal Ureña, J. R. Avilés Moreno, I. Mata, E. Molins, R. M. Claramunt, C. López, I. Alkorta, J. Elguero, *New J. Chem*. **2012**, *36*, 749.

[6] L. Pérez-García, D. B. Amabilino, *Chem. Soc. Rev.*, **2002**, *31*, 342.

[7] a) F. Partal Ureña, J. R. Avilés Moreno, J. J. López González, *J. Phys. Chem. A*. **2008**, *112*, 7887; b) J. R. Avilés Moreno, F. Partal Ureña, J. J. López González, *Phys. Chem. Chem. Phys.* **2009**, *11*, 2459; c) J. R. Avilés Moreno, M. M. Quesada Moreno, F. Partal Ureña, J. J. López González, *Tetrahedron: Asymmetry* **2012**, *23*, 1084; d) T. R. Huet, J. R. Avilés Moreno, O. Pirali, M.

Tudorie, F. Partal Ureña, J. J. López González, *J. Quant. Spectrosc. Radiat. Transfer*. **2012**, *113*, 1261; e) F. Partal Ureña, J. R. Avilés Moreno, J. J. López González, *Chirality*. **2010**, *22*, E123; f) J. R. Avilés Moreno, F. Partal Ureña, J. J. López González, *Asian J. Spectrosc.* **2010,** *14*, 1.

[8] a) S. Graus, R. M. Tejedor, S. Uriel, J. L. Serrano, I. Alkorta, J. Elguero, *J. Am. Chem. Soc*., **2010**, *132*, 7862; b) J. R. Avilés Moreno, J. J. López González, F. Partal Ureña, F. Vera, M. B. Ros, T. Sierra, *J. Phys. Chem. B*, **2012**, *116*, 5090; c) R. M. Tejedor, L. Oriol, J. L. Serrano, F. Partal Ureña, J. J. López González, *Adv. Funct. Mater.* **2007**, *17*, 3486.

[9] a) A. Llamas-Saiz, C. Foces-Foces, I. Sobrados, J. Elguero, W. Meutermans, *Acta Crystallogr. Sect. C.* **1993**, *49*, 724; b) M. M. Quesada Moreno, J. R. Avilés Moreno, J. J. López González, R. M. Claramunt, C. López, I. Alkorta, J. Elguero. *Tetrahedron: Asymmetry*, sent for publication in March 2013.

[10] NIST Standard Reference Database 101; Computational Chemistry Comparison and Benchmark DataBase: http://cccbdb.nist.gov/vibscalejust.

[11] I. Alkorta, J. Elguero, C. Roussel, *Tetrahedron: Asymmetry* **2011**, *22*, 1180.

[12] T. B. Freedmand, X. Cao, D. A. Young, L. A. Nafie, *J. Phys. Chem. A* **2002**, *106*, 3560.

[13] V. P. Nicu, J. Autschbach, E. J. Baerends, *Phys. Chem. Chem. Phys*. **2009**, *11*, 1526.

[14] V. P. Nicu, M. Heshmath, E. J. Baerends, *Phys. Chem. Chem. Phys*. **2011**, *13*, 8811.

[15] a). Ch. Ruechardt, V. Hassmann, H.-J. Quadbeck-Seeger, H. Armbrust, Badische Anilin & Soda-Fabrik Jan, 28 **1975**: US Patent 3862958; b) R. Huisgen and K. Bast, Org. Synth. 1962, 42, 69.

[16] R. Kuroda, T. Harada, Y. Shindo, *Rev. Sci. Instrum.* **2004**, *72*, 3802.

[17] C. Merten, T. Kowalik, A. Hartwig, *Appl. Spectrosc*. **2008**, *62*, 901.

[18] T. Buffeteau, F. Lagugné-Labarthet, C. Sourisseau, *Appl. Spectrosc*. **2005**, *59*, 732.

[19] a) A. D. Becke, *Phys. Rev. A: At. Mol. Opt. Phys.* **1988**, *38*, 3098; b) A. D. Becke, *J. Chem. Phys.* **1993**, *98*, 5648; c) C. Lee, W. Yang, R. G. Parr, *Phys. Rev. B* **1988**, *37*, 785.

[20] P. A. Hariharan, J. A. Pople, *Theor. Chim. Acta* **1973**, *28*, 213.

[21] Gaussian09, M. J. Frisch *et al*., Gaussian Inc., Wallingford CT, **2010**.

Supporting information

Self-assembly structures of 1*H*-indazoles in solution and solid phases: A vibrational (IR, FarIR, Raman and VCD) and computational study.

J. R. Avilés Moreno,[a] M. M. Quesada Moreno, [a] J. J. López González,*[a] R. M. Claramunt,*[b] C. López, [b] I. Alkorta[c] and J. Elguero*[c]

[a] *Departamento de Química Física y Analítica, Universidad de Jaén, Campus Las Lagunillas, E-23071 Jaén, Spain*
E-mail: jjlopez@ujaen.es

[b] *Departamento de Química Orgánica y Bio-Orgánica, Facultad de Ciencias, Universidad Nacional de Educación a Distancia (UNED), Senda del Rey 9, E-28040 Madrid, Spain*
E-mail: rclaramunt@ccia.uned.es

[c] *Instituto de Química Médica (CSIC), Juan de la Cierva, 3,E-28006 Madrid, Spain*
E-mail: iqmbe17@iqm.csic.es

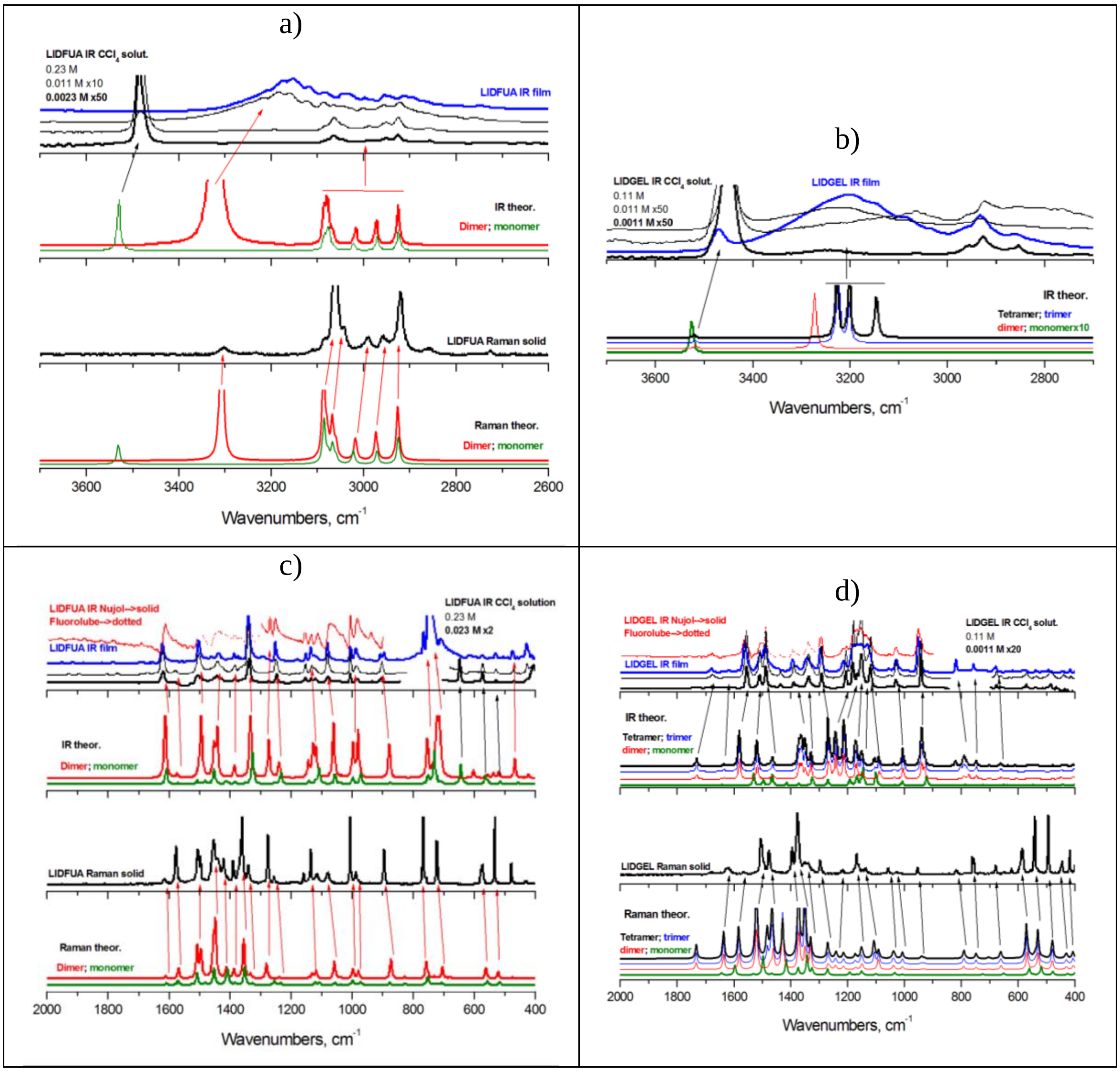

Figure 1S. Experimental and scaled predicted IR (top) and Raman (bottom) spectra of **LIDFUA** (panels a and c) and **LIDGEL** (panels b and d) in the 3700 cm^{-1}–2600 cm^{-1} and in the 2000-400 cm^{-1} spectral regions.

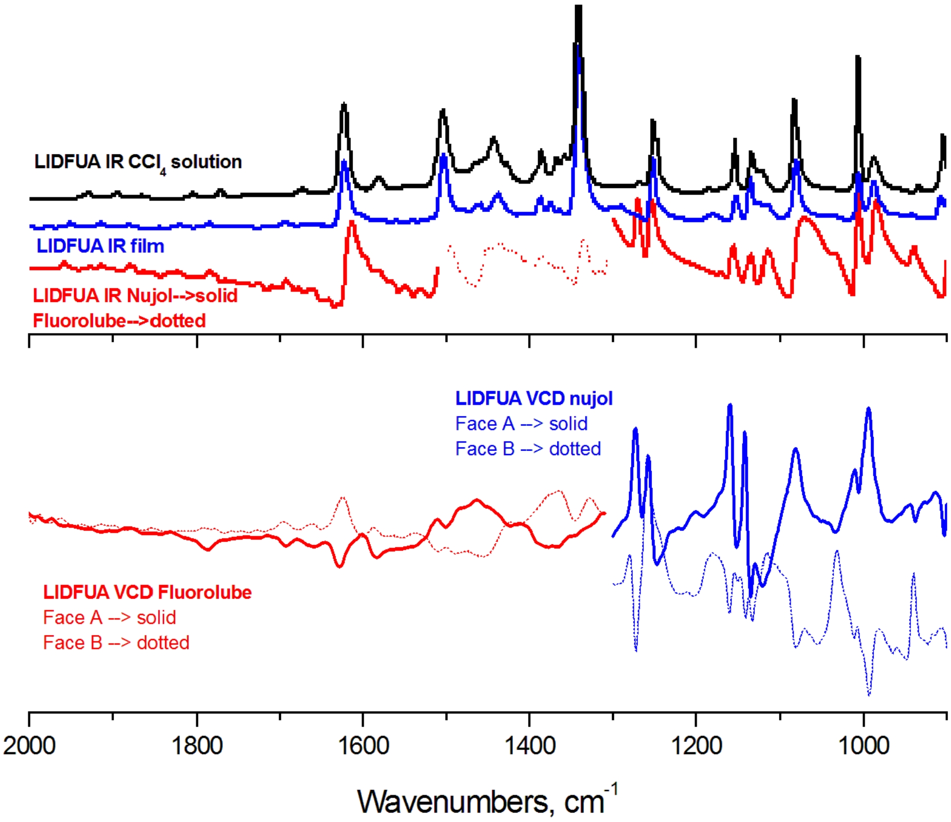

Figure 2S. Experimental IR (top) and VCD (bottom) spectra of **LIDFUA** in fluorolube and nujol mulls for faces A and B (rotation of 180º with respect to the perpendicular axis to the beam propagation) in the 2000 cm^{-1}–900 cm^{-1} spectral region.